Proceedings World Geothermal Congress 2026
Calgary, Canada, June 8 – 11, 2026

Modelling and Optimization Design of a Western Canadian Geothermal Aquifer Flow System: A Case Study

S. Maaref[1]*, A. Shariat [1], K. Joslin[1], M. Eyre [2], and T. Thompson[3]
Computer Modelling Group Ltd.[1], Barkley Project Group[2], Borealis GeoPower Inc.[3]

*Sepideh.maaref@cmgl.ca

ABSTRACT

Geothermal energy plays a vital role in advancing a sustainable, low-carbon economy. Developing geothermal resources can be achieved through water circulation between injection wells, thermal reservoir, and production wells, providing an economically viable means to extract earth's thermal energy. This study evaluates and optimizes the heat production efficiency of a high-temperature Western Canadian geothermal aquifer system under various well design scenarios. The geothermal aquifer flow is modeled using a thermal numerical reservoir simulator, coupled with a semi-analytical wellbore model. The heat production efficiency is examined by analysis of maximum attainable flow rates, produced fluid temperature profiles, and thermal breakthrough behavior. A key focus is optimizing producer pump depth to effectively lift high-density brine from deep formation while minimizing operational costs. Additionally, the impact of injection wellhead pressure on system performance is analyzed. The findings indicate the complex role of reservoir permeability heterogeneity in optimizing well configurations, thermal breakthrough, pump depth, and wellhead pressures. A key trade-off is managing injection wellhead pressure and the required pump depth for the producer. Reducing injection wellhead pressure will necessitate a deeper pump on the producer side, while higher injection pressure requires a shallower pump location. The choice between these scenarios is underscored by multiple factors, including reservoir permeability, economics, achieving the desired flow rate, target producer surface temperature, thermal breakthrough time, and targeted thermal power. These insights contribute to a deeper understanding of geothermal system dynamics and provide valuable guidance for optimizing geothermal energy extraction in a cost effective and sustainable manner.

1 INTRODUCTION

Geothermal energy is a clean, renewable alternative energy source which has been utilized for power generation and direct heating applications [1-5]. Geothermal resources are categorized into conventional and unconventional types, based on their natural properties [6]. Conventional geothermal resources have the essential characteristics for energy extraction including sufficient heat, natural permeability, and the presence of fluids [7, 8]. These conditions allow energy to be harnessed through well systems without the need for enhanced techniques such as hydraulic fracturing (as in Enhanced Geothermal Systems (EGS)) or closed-loop systems.

Common well configurations in conventional geothermal resources include single-well systems [9-11] and multi-well layouts, such as doublets, triplets, or five-spot arrangements [12-14]. In these designs, cold water is injected into one or more wells, while hot water or steam is extracted from others [15]. Reinjection of geothermal fluids into the reservoir is a proven method for extending the productive life of geothermal systems and enhancing thermal energy recovery. This process maintains reservoir pressure, mitigates production decline, and extends the operational lifespan of the reservoir [16, 17]. However, poorly managed reinjection can lead to adverse effects such as early thermal breakthrough, where cold injected fluids prematurely cool down production zones, reducing energy recovery and affecting the long-term sustainability [18].

Effective geothermal field development is complicated and maximum geothermal energy recovery depends on optimal well configuration, operational conditions and reservoir properties [19-22]. This includes recognizing the key subsurface characteristics that govern reservoir performance, as well as the operational strategies that affect energy extraction over time. From a physical standpoint, reservoir properties such as permeability, thermal conductivity, and temperature influence the amount of thermal energy available [23-25]. The spatial distribution of these properties further affects how efficiently heat can be extracted and sustained over the lifespan of a geothermal project. Equally important are operational factors, including well design and spacing, injection and production rates and temperatures [26-30]. These parameters control the dynamics of heat extraction. For example, increasing the mass flow rate may initially enhance production, but can lead to rapid declines in outlet temperature [31]. Conversely, certain strategies such as injecting lower-temperature fluids have been shown to yield higher heat outputs under specific conditions [32, 33]. Carefully optimizing these variables is crucial to maximizing energy recovery while minimizing the risks of thermal breakthrough and pressure depletion [1].

Given the complexity of managing geothermal energy systems, this study aims to optimize the well configuration to maintain high flow rates and stable delivery temperatures for at least 20 years. The study will also assess thermal breakthrough, optimal pump set depth and injection well head pressure, and evaluate the impact of well configuration (e.g., producer well length and well pair spacing) and operational conditions (e.g., production/injection delay and casing size). Optimizing pump depth is particularly crucial to effectively lift high-density brine while minimizing operational costs by reducing energy consumption and wear on equipment. By examining these factors, the study aims to enhance the efficiency, sustainability, and operational longevity of geothermal energy extraction.

2 GEOTHERMAL RESERVOIR DESCRIPTION

This study evaluated the potential of a Western Canadian geothermal aquifer. The reservoir presents a promising geothermal resource with a temperature range of 102 °C to 140 °C. The reservoir is characterized by two distinct sandstone (SS) formations as shown in **Figure** 1.

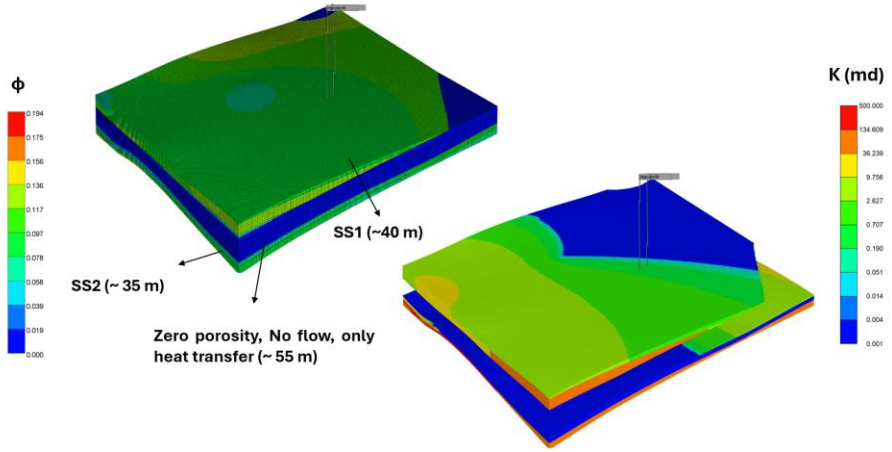


Figure 1. Geothermal reservoir structure, porosity, and permeability.

These formations are separated by an impermeable shale layer of zero porosity (~55 m). While the two sandstone formations do not exhibit any direct flow communication, conductive heat transfer is modelled between them. The reservoir permeability is heterogeneous, with high permeability zones adjacent to low permeability areas (see **Figure** 1). Detailed reservoir properties are provided in **Table** 1.

Table 1. Geothermal reservoir properties.

Model Dimension	48 km × 48 km × 0.13 km
Average Porosity	0.047
Average Horizontal Permeability	47 md
Average Vertical permeability	24 md
Aquifer Brine Density	1188 kg/m^3
Sandstone Thermal conductivity	3.31 W/(m.K)
Sandstone Volumetric Heat capacity	4.26 ×10^6 J/(m^{3}K)
Shale Thermal conductivity	1.25 W/(m.K)
Shale Volumetric Heat capacity	4.51 ×10^6 J/(m^{3}K)
Average Temperature Gradient	32 °C/km
Overburden/Underburden Volumetric Heat Capacity	4.26 ×10^6 J/(m^{3}K)
Overburden/Underburden Thermal Conductivity	3.31 W/(m.K)
Heat Flux	70 mW/m^2

The reservoir pressure at the well location is approximately 31.3 MPa, and the brine density is about 1188 kg/m^3. Even in the absence of flow and frictional pressure drop, the reservoir pressure alone is insufficient to naturally produce the high-density brine from a depth of 3000 m to the surface (see **Figure 2 (b)**). Thus, a key challenge in this study is the requirement and location of a pump in the producer well. This necessitates careful wellbore design and evaluation of various operational conditions to optimize the pump set depth.

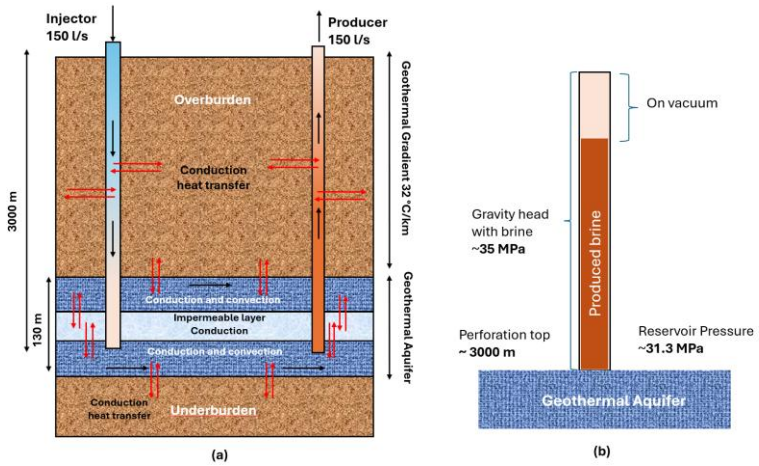
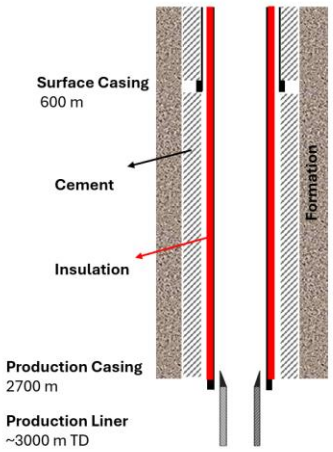


Figure 2. (a) Schematic of the conventional geothermal aquifer flow system, and (b) schematic of producer wellbore in absence of any fluid flow and frictional pressure drop, lifting the fluid with gravity only.

3 METHODOLOGY

3.1 Base Case Model

The geothermal aquifer flow is modeled using a thermal numerical reservoir simulator, coupled to a semi-analytical wellbore model. The system is configured as a conventional geothermal setup with water circulation between injection well, thermal formation, and production well (see **Figure 2 (a)**). To evaluate the geothermal potential, a parallel horizontal well pair was considered. The wellbore is modeled using a Semi-Analytical Modeling (SAM) approach. With the SAM model, pressure drop along the wellbore and radial heat loss from a wellbore is calculated semi-analytically based on Fontanilla and Aziz [34], where momentum and energy equations are solved simultaneously to evaluate pressure and enthalpy changes along the wellbore. The wellbore schematic including surface casing and production casing dimensions, along with their thermal properties, are specified in **Figure 3**. The wellbore flow is assumed to be mainly from the production casing (ID: 228.6 mm) extending from ~3000 m depth to the surface. Radial Heat loss from wellbore is calculated using dimensions and thermal properties of surface casing, production casing, insulation, cement, and formation.



Wellbore	Surface Casing	Production Casing	Production Liner	Insulation	Cement
From Depth (mKB)	0	600	2700	0	0
To Depth (mKB)	600	2700	TD (~ 3000)	TD (~ 3000)	TD (~ 3000)
ID (mm)	376.5	228.6	161.7	NA	406
OD (mm)	406	244.5	177.8	NA	508
Thickness (mm)	14.75	7.95	8.05	10	51
Thermal Conductivity (J/m.day.°C)	3738000	3738000	NA	777.6	30240
Emissivity	0.8	0.8	NA	0.9	NA
Relative Roughness	0.0001	0.0001	NA	NA	NA

Figure 3. Wellbore schematic, dimensions and thermal properties.

In the base model, formation brine is re-injected at a temperature of 85 °C and a rate of 150 l/s, with the hot formation brine being produced at the same rate. Brine density and viscosity are modeled as functions of pressure and temperature at a salinity of 250 mg/L. A maximum bottom hole pressure (BHP) limit of ~48.6 MPa is set for the injector. A pump was also modelled inside the production well to facilitate fluid production.

The horizontal configuration maintained the full flow rate of 150 l/s for the entire 20 years before reaching the maximum BHP. The required pump set depth in the base case was determined based on the producer minimum BHP compared to the wellbore pressure drop. As shown in **Figure 4**, total pressure drop in the wellbore including

both friction and gravity is 36.6 MPa, and the minimum producer BHP is 23.5 MPa. Consequently, the pump must be placed at a depth of at least 1100 m to lift the high-density brine (1188 kg/m3) to the surface.

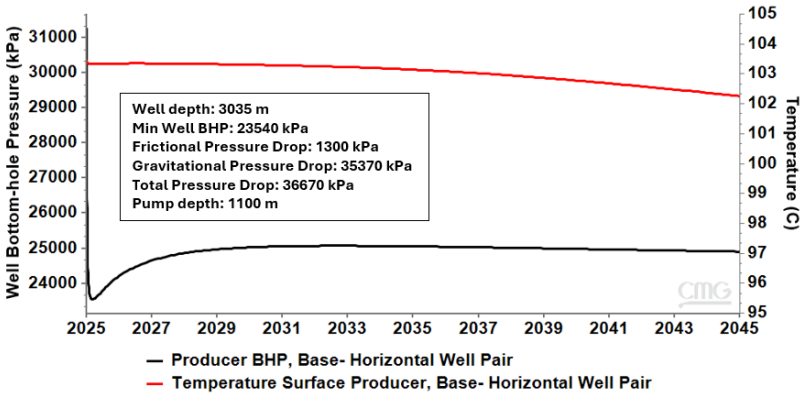


Figure 4. Producer well bottom hole pressure, pump depth, and produced water temperature for horizontal well configuration.

Figure 4 also shows the producer's surface temperature over time in red. **Figure 5** shows the temperature profile between the horizontal well pair at 0, 5, 10, and 20 years. Both figures suggest that the thermal breakthrough occurred at ~10 years, resulting in a reducing trend in surface temperature. However, the surface temperature still remained above 102 °C throughout the 20-year period for the horizontal well pair. It is also notable that the producer bottomhole temperature is around 110 °C after 20 years, while it's 102 °C at the producer surface. This is related to the wellbore heat loss to the formation and is affected by insulation thickness and thermal properties (see **Figure 3**).

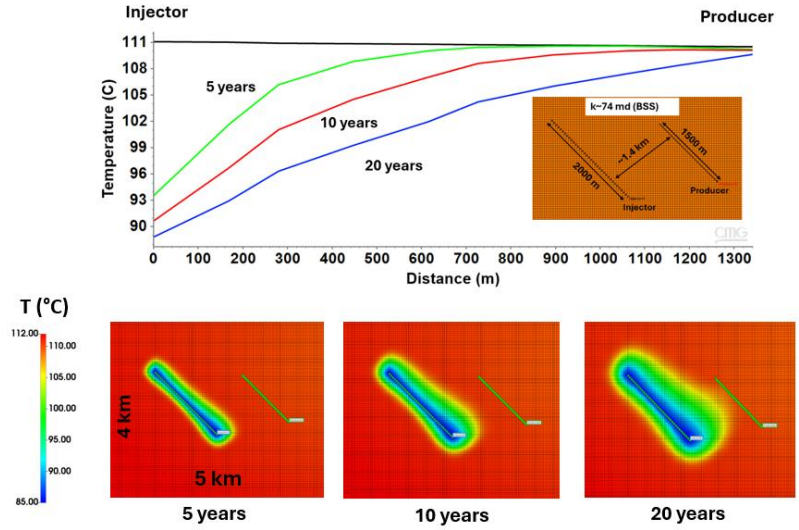


Figure 5. Temperature profile between the horizontal injector and producer at initial, 5 years, 10 years, and 20 years of geothermal operation.

3.2 Optimization Scenarios

While the base case maintains a high circulation flow rate (150 l/s) and temperature (>100°C) over a 20-year period, the pump set depth of 1100 m is considered deep, leading to increased operational costs. Therefore, further optimization is required to reduce the pump set depth while maintaining system efficiency and performance. To optimize the pump set depth, a sensitivity analysis was performed on several operational conditions and wellbore configurations, including: Producer well length- Case 1 (3.7 km producer), Production delay, Step rate increase- Case 2 (75 l/s for 2 yrs, 150 l/s for 18 yrs), Second producer after 10 years- Case 3, Well pair spacing- Cases 4, 4a, 4b (1400 m, 1000 m, and 850 m), and Production casing size- Case 5 (ID: 322.6 mm). By adjusting these parameters, the goal is to reduce the pump depth while ensuring that the system continues to meet the required flow rates and temperatures. In all cases, brine is re-injected at 85 °C.

4 RESULTS AND DISCUSSION

The effect of each sensitivity analysis on the pump depth saving while maintaining the rate and delivery temperature is discussed below.

4.1 Producer well length

In this case, the producer well length is increased from 1.5 km to 3.7 km, and the production rate is maintained at 150 l/s. By increasing the well length, the larger contact area with the reservoir reduces pressure drawdown, which results in a higher BHP compared to the base case configuration. This increase in BHP allows for a more efficient production system, which leads to pump depth saving. Here, increasing the producer well length from 1.5 km to 3.7 km resulted in an estimated pump depth saving of approximately 330 m. The breakdown of frictional and gravitational pressure drops relative to the BHP is also shown in **Figure 6**.

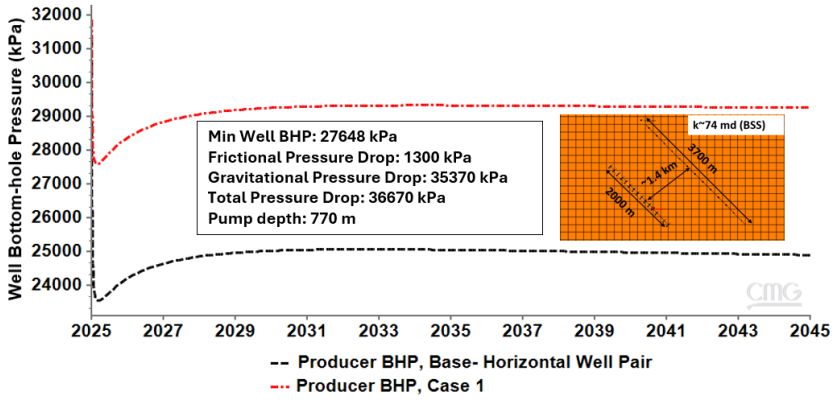


Figure 6. Effect of producer well length on producer well bottom hole pressure and pump depth.

4.2 Production delay

4.2.1 Step rate increase

In this operational scenario, both the injector and producer operate at half rate (75 l/s) for the first 2 years, followed by full rate production (150 l/s) for the next 18 years. Circulating the fluid at half rate during the initial 2 years resulted in less drawdown and higher bottomhole pressure (BHP) for the producer as shown in **Figure 7**. When the injection rate increases to full rate after 2 years, the BHP drops; however, the decline is not as significant as in the base case scenario. This is because the pressure support from the injector has already been established during the initial phase at the half rate. This operational strategy helps mitigate pressure drop, leading to an additional pump depth saving of approximately 100 m.

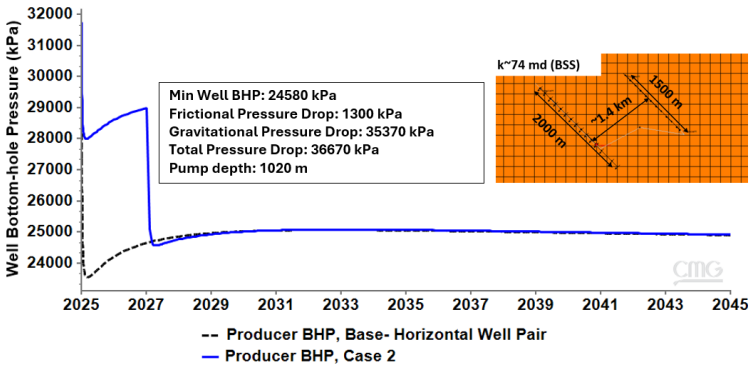


Figure 7. Effect of production delay (step rate increase) on producer well bottom hole pressure and pump depth.

4.2.2 2nd producer

This scenario involves an injector located between two producers. The aim was to take advantage of pressure propagation on both sides of the injector. Initially, the first well pair (injector and producer-1) operate at full rate of 150 l/s for 10 years. After 10 years, the first producer is shut in, and a second producer is brought online on the opposite side of the injector, operating at full rate as well.

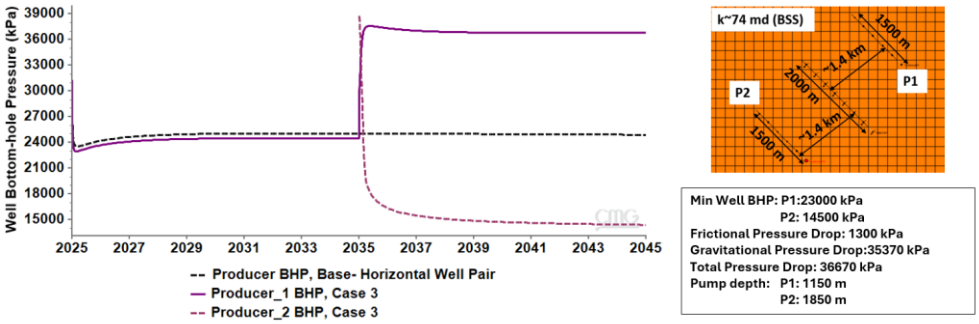


Figure 8. Effect of production delay (2nd producer after 10 yrs.) on producer well bottom hole pressure and pump depth.

Adding the second producer proved beneficial in terms of injector-side pressure management; however, it resulted in a larger BHP decline at Producer 2 due to the reservoir heterogeneity. At the location of the second producer, the thickness of the formation with favorable permeability is reduced by approximately 50%. As a result, the second producer experiences limited inflow capacity despite the elevated reservoir pressure by the injector. This highlights the critical influence of reservoir permeability distribution on the effectiveness of well placement and delayed production strategies.

4.3 Well pair spacing

Figure 9 compares the effect of three different well spacing of 1400 m, 1000 m, and 850 m on pump depth saving. Reducing the well spacing from 1400 m to 850 m enhanced pressure support, resulting in higher BHP on the producer side and further pump depth savings of approximately 120 m. However, a reduction in well spacing also leads to earlier thermal breakthrough. This introduces a trade-off between pump depth savings and long-term thermal sustainability. Therefore, well spacing must be optimized based on the desired thermal breakthrough time. A thermal breakthrough time of 10 years was selected as the operational target and a well spacing of 1000 m was identified as the optimal distance, achieving the desired 10-year thermal breakthrough while maintaining surface temperatures above 102°C throughout the 20 years operational period.

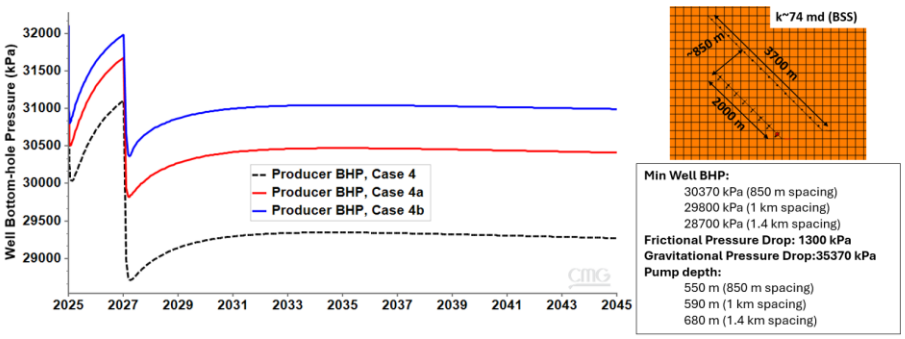


Figure 9. Effect of well pair spacing on producer well bottom hole pressure and pump depth.

4.4 Production casing size

Increasing the production casing size resulted in a reduced frictional pressure drop along the vertical section to 244 kPa, which in turn reduced the total pressure drop in the wellbore. With the same BHP on the producer well, this decrease in pressure drop led to an approximate 100 m depth saving when increasing the production casing ID from 228.6 mm to 322.96 mm.

4.5 Pump Depth Summary and Produced Surface Temperatures

The analysis of different operational conditions resulted in the following breakdown of pump depth savings from 1100 m to 490 m: producer well length (increased from 1.5 km to 3.7 km) led to a reduction of ~330 m in pump depth, production delay (with half-rate followed by full-rate) contributed to a reduction of ~100 m, well spacing (decreasing from 1,400 m to 850 m) helped reduce depth by ~120 m, and well diameter (increasing the

production casing ID from 228.6 mm to 322 mm) resulted in a ~100 m decrease in depth. It is notable that the produced water surface temperatures for cases 1 to 5 are maintained above 100 °C for all cases.

4.6 Injector Well Head Pressure Sensitivity

Although case 5 showed the minimum pump depth on the producer side, the injector WHP should be also monitored for optimized operation. **Figure 10** shows the injector wellhead pressure (WHP) for case 5.

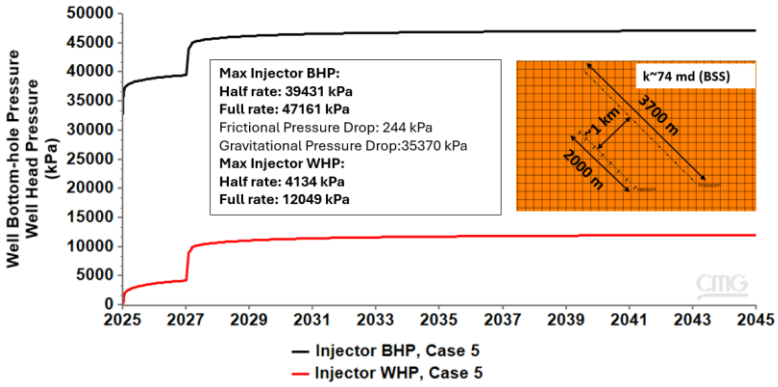


Figure 10. Injector well head pressure and bottom hole pressure of Case 5.

At half rate, the injector WHP is 4134 kPa, and at full rate, it increases to 12049 kPa. To achieve this, the fluid needs to be pumped at ~12 MPa at the wellhead, which poses several challenges. High pressure pumping can lead to substantial increases in both capital and operational costs.

To address the high injector WHP, further sensitivity analysis is performed to evaluate ways to reduce the injector WHP. The sensitivity analysis on the injector WHP is done by adjusting several operational parameters including: lowering the fluid circulation rate- Case 6 (75 l/s for 20 yrs), performing hydraulic fracturing in the injector- Case 7, dividing the injection rate between two injectors- Case 8 (37.5 l/s for 2 yrs, 75 l/s for 18 yrs per injector, and decreasing the well length- Case 8a (1.4 km Injector). It is notable that in all sensitivity cases, the producer pump depth was adjusted for optimized conditions, and efforts were made to maintain the same delivery temperature and thermal breakthrough dynamics, ensuring that these adjustments do not compromise produced thermal energy sustainability.

4.6.1 Injection Rate

Figure 11 shows that lowering the injection rate to 75 l/s resulted in the injection wellhead pressure (WHP) reduction from 12 MPa to 5 MPa. Moreover, a lower circulation rate led to a smaller pressure drop within the reservoir. This resulted in additional pump depth savings and reduced the pump depth to 430 m. Balancing the WHP reduction with flow rate targets will be important for long term sustainability and thermal power generation.

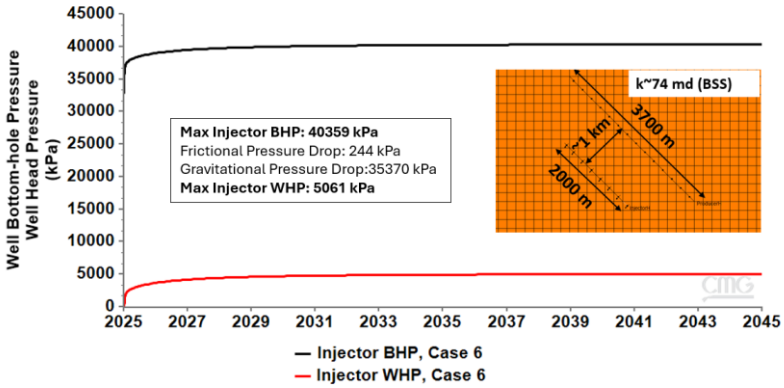


Figure 11. Effect of injection rate on injector well head pressure and bottom hole pressure.

4.6.2 Injector with Hydraulic fracture

In this scenario, 8 hydraulic fractures were modeled for the injection well. Hydraulic fracturing enhanced injectivity by creating additional pathways for fluid flow within the injector well. This resulted in a reduction of the required wellhead pressure (WHP) for fluid injection, lowering it to 2.4 MPa at half rate (75 l/s) and 8.4 MPa at full rate (150l/s). However, hydraulic fracturing introduces additional operational complexities and risks, including potential reservoir damage, increased seismicity, and higher costs. The decision to implement hydraulic fracturing versus optimizing the pump cost depends on a detailed economic analysis, weighing the costs of fracturing against the potential savings in pump power and long-term operational benefits.

4.6.3 Injection Delay_2nd injector

This case employs a configuration with one producer in the middle and two injectors on either side. The injection rate is divided between the two injectors, with each injector operating at quarter (37.5 l/s each) and half (75 l/s each) of the total rate (150 l/s). **Figure 12** illustrates the injector wellhead pressure (WHP), showing that Injector 1 and 2 goes into a vacuum state at 37.5 l/s. As the injection rate doubles, about 1.5 MPa wellhead pressure is required for Injector 1. Injector 2, on the other hand, requires a well head pressure of 4.3 MPa at the half rate. **Figure 13** also suggests that the pump should be placed at 650 m. This configuration successfully decreased the WHP at the injectors compared to case 5 but resulted in a higher pump depth location due to the less pressure support from the injection wells. To further optimize the system and reduce costs, additional adjustments were made to the length of the injectors.

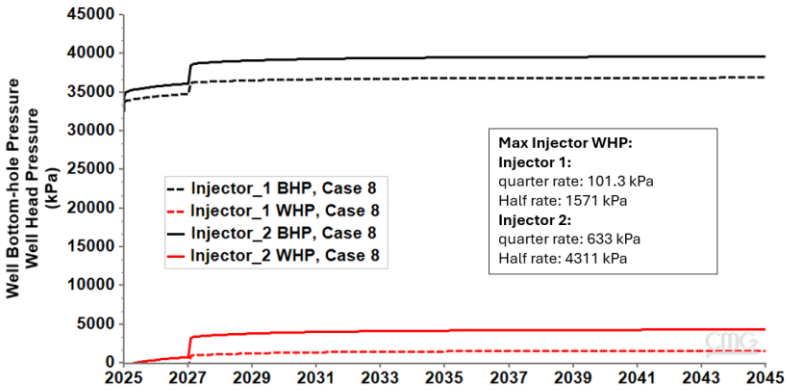


Figure 12. Effect of injection rate division with less well spacing on injector well head pressure and bottom hole pressure.

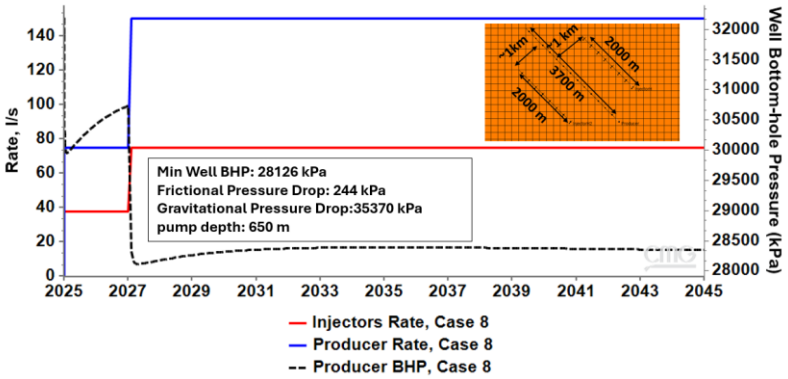


Figure 13. Well pair water circulation rate and producer bottom hole pressure along with pump depth for case 8.

4.6.4 Injection Delay _2nd injector_ Well Length

Figure 14 shows that decreasing the horizontal injector well length from 2 km to 1.4 km led to a higher injector wellhead pressure (WHP) due to a reduction in well injectivity. Despite this, the producer pump depth remained the same as in case 8, at 650 m. This change resulted in a 600 m saving in the length of each horizontal injector but also caused an increase in the injector WHP to 3 MPa and 6.7 MPa for injectors 1 and 2, respectively. Since

the producer pump depth stayed consistent with that of case 8, the decision to implement this change depends on the operational preference regarding the wellhead injection pressure.

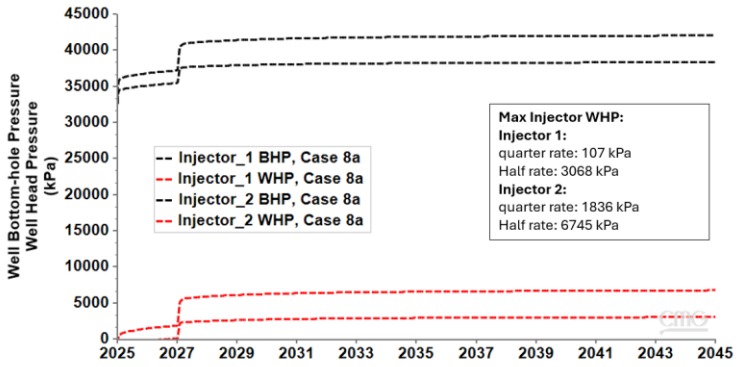


Figure 14. Effect of injection rate division with less well spacing and well length on injector well head pressure and bottom hole pressure.

4.6.5 Injection Wellhead Pressure Summary

Table 2 summarizes the wellhead pressure (WHP) and pump depth savings under different operational conditions. **Table 3** also compares the injection and production temperature, well head pressure, and net thermal power under different operational conditions. Net thermal power is calculated as the product of flow rate and enthalpy difference between the injected and produced water. All the scenarios show liquid hot water production at the surface with temperatures above 100 °C. The difference comes from different flow rates that resulted in a net thermal power of ~6-7 MWth at half rate of 75 l/s and 12-14 MWth at full rate of 150 l/s. Additional differences arise from variations in pump depth and required injection wellhead pressure.

Table 2. Summary of WHP and pump depth saving at different operational conditions.

Case	Sensitivity Analysis	Injector WHP (kPa)	Producer Pump Depth (m)
5	Base	Half rate: 4134, full rate: 12049	490
6	Injection rate	5061	430
7	Injector with hydraulic fracture	Half rate: 2474, full rate: 8456	490
8	Injection delay_2nd injector_Step rate	**Injector 1:** quarter rate: 101.3, half rate: 1571 **Injector 2:** quarter rate: 633, half rate: 4311	650
8a	Injection delay_2nd injector_Step rate/ Well length	**Injector 1:** quarter rate: 107, half rate: 3068 **Injector 2:** quarter rate: 1836, half rate: 6745	650

Table 3. Injection and production temperature, injection pressure, and net thermal power for cases 5 to 8a.

Case	Q (l/s)	Pinj (KPa)	Tinj (°C)	Tprod (°C)	Net Thermal Power (MW_{th})	Duration (Years)
5	75	4134	85	102.6	6.74	2
	150	12049	85	101.9	11.66	18
6	75	5061	85	102.9	6.59	20
7	75	2474	85	103.3	6.85	2
	150	8456	85	102.4	12.30	18
8	75	Inj-1 (37.5 l/s): 101.3	85	103.9	7.29	2
		Inj-2 (37.5 l/s): 1571	85			
	150	Inj-1 (75 l/s): 633	85	103.4	14.10	18
		Inj-2 (75 l/s): 4311	85			
8a	75	Inj-1 (37.5 l/s): 107	85	103.9	7.30	2
		Inj-2 (37.5 l/s): 3068	85			
	150	Inj-1 (75 l/s): 1836	85	103.2	13.80	18
		Inj-2 (75 l/s): 6745	85			

The choice of the best scenario depends on the technical limitations and operational costs incorporating desired wellhead pressure (WHP), pump depth, wellbore dimensions, and target thermal power.

Among the tested configurations, the most promising setup in terms of pump depth and injector wellhead pressure involved reducing the fluid circulation rate to half rate (75 l/s) while using one injector and one producer. This configuration resulted in a WHP of 5 MPa and a pump depth of 430 m. However, lowering the rate resulted in lowering the net thermal power to 6.6 MWth. In the case of a full injection rate (150 l/s), the optimal configuration would involve two injectors (each operating at half the rate) and one producer (operating at full rate). In this case, the maximum WHP varied between 4 MPa and 6.7 MPa depending on well length, with a pump depth of 650 m on the producer side. Moreover, the corresponding net thermal power was 7.3 MWth at half rate and 14 MWth at full rate. Ultimately, the choice of configuration and circulation rate depends on the added benefit in terms of thermal power versus the capital and operational costs of an extra horizontal well and a higher capacity production pump.

5 CONCLUSIONS

This study investigated various well configurations and operational strategies to optimize a conventional geothermal production system. The goal was to minimize pump depth and wellhead pressure (WHP) while sustaining a flow rate of 150 l/s and temperatures above 100 °C over 20 years. Key optimizations were achieved through adjustments to the horizontal well pair, including increasing producer well length, delaying production, reducing well spacing, and increasing casing size. These changes resulted in significant reductions in pump depth, from 1100 m to 490 m.

Despite improvements, the minimum pump depth scenario still required a well head pressure (WHP) of 12 MPa. Sensitivity analysis showed that reducing injector WHP further necessitated operational changes such as lowering circulation rate, hydraulic fracturing, splitting the injection between two wells, or changing injector length. However, reducing the WHP also led to the need for a deeper pump (~650 m), as the lower injection pressure decreased reservoir support and bottomhole pressure (BHP).

Among the configurations tested, the most favorable low-rate setup used one injector and one producer at 75 l/s, achieving a WHP of 5 MPa, pump depth of 430 m, and net thermal output of 6.6 MW_{th}. However, this lower thermal output may not meet energy demands. At double injection rate (150 l/s), the optimal setup included two injectors at half capacity and one full-capacity producer, yielding 7.3 MW_{th} at half rate and 14 MW_{th} at full rate. This required a deeper pump (650 m) and WHP between 4-7 MPa, depending on the injector length.

The operational strategies examined in this study were heavily influenced by the permeability distribution in the reservoir and the specific constraints of the permitted area. Therefore, the decision-making process must account for both the technical and economic factors. The findings highlight the importance of balancing reservoir conditions, well configuration, and operational costs to design efficient, sustainable geothermal systems tailored to site-specific constraints.

REFERENCES

1. Song, G.; Song, X.; Li, G.; Shi, Y.; Wang, G.; Ji, J.; Xu, F.; Song, Z., An integrated multi-objective optimization method to improve the performance of multilateral-well geothermal system. Renewable Energy 2021, 172, 1233-1249.
2. Sims, R. E., Renewable energy and climate change mitigation: an overview of the IPCC Special Report. Weather matters for energy 2014, 91-110.
3. Panwar, N. L.; Kaushik, S. C.; Kothari, S., Role of renewable energy sources in environmental protection: A review. Renewable and sustainable energy reviews 2011, 15 (3), 1513-1524.
4. Lund, J. W.; Boyd, T. L., Direct utilization of geothermal energy 2015 worldwide review. Geothermics 2016, 60, 66-93.
5. Chen, H.; Shi, Y.; Liu, C.; Zhao, Z.; Yue, Y.; Li, M., Performance comparison of different well configurations for medium-deep coaxial closed-loop geothermal systems. Applied Thermal Engineering 2025, 126393.
6. Khodayar, M.; Björnsson, S., Conventional geothermal systems and unconventional geothermal developments: An overview. Open Journal of Geology 2024, 14 (02), 196-246.
7. Muffler, P.; Cataldi, R., Methods for regional assessment of geothermal resources. Geothermics 1978, 7 (2-4), 53-89.
8. Williams, C. F.; Reed, M. J.; Anderson, A. F. In Updating the classification of geothermal resources, Proceedings, Thirty-Sixth Workshop on Geothermal Reservoir Engineering, 2011; p 7.
9. Bu, X.; Ran, Y.; Zhang, D., Experimental and simulation studies of geothermal single well for building heating. Renewable Energy 2019, 143, 1902-1909.
10. Falcone, G.; Liu, X.; Okech, R. R.; Seyidov, F.; Teodoriu, C., Assessment of deep geothermal energy exploitation methods: The need for novel single-well solutions. Energy 2018, 160, 54-63.
11. Xu, T.; Li, F.; Feng, B.; Feng, G.; Jiang, Z., Numerical evaluation of the performance of a single-well groundwater source heat pump system in Beijing, China. Energy Exploration & Exploitation 2020, 38 (1), 201-221.
12. Li, F.; Xu, T.; Li, S.; Feng, B.; Jia, X.; Feng, G.; Zhu, H.; Jiang, Z., Assessment of Energy Production in the Deep Carbonate Geothermal Reservoir by Wellbore-Reservoir Integrated Fluid and Heat Transport Modeling. Geofluids 2019, 2019 (1), 8573182.
13. Asai, P.; Panja, P.; McLennan, J.; Deo, M., Effect of different flow schemes on heat recovery from Enhanced Geothermal Systems (EGS). Energy 2019, 175, 667-676.
14. Chen, J.; Jiang, F., Designing multi-well layout for enhanced geothermal system to better exploit hot dry rock geothermal energy. Renewable Energy 2015, 74, 37-48.
15. Li, F.; Guo, X.; Qi, X.; Feng, B.; Liu, J.; Xie, Y.; Gu, Y., A Surrogate Model-Based Optimization Approach for Geothermal Well-Doublet Placement Using a Regularized LSTM-CNN Model and Grey Wolf Optimizer. Sustainability 2025, 17 (1), 266.
16. Chen, M.; Tompson, A. F.; Mellors, R. J.; Abdalla, O., An efficient optimization of well placement and control for a geothermal prospect under geological uncertainty. Applied energy 2015, 137, 352-363.
17. Stefansson, V.-đ., Geothermal reinjection experience. Geothermics 1997, 26 (1), 99-139.
18. Liu, Y.; Guo, L.; Wang, Y.; Liao, Y.; Zhao, G., Numerical simulation and design optimization of large-scale geothermal production based on a multiwell layout in xianxian geothermal field. Lithosphere 2022, 2021 (Special 5), 2929551.
19. Procesi, M.; Cantucci, B.; Buttinelli, M.; Armezzani, G.; Quattrocchi, F.; Boschi, E., Strategic use of the underground in an energy mix plan: Synergies among CO2, CH4 geological storage and geothermal energy. Latium Region case study (Central Italy). Applied Energy 2013, 110, 104-131.
20. Kaniyal, A. A.; Nathan, G. J.; Pincus, J. J., The potential role of data-centres in enabling investment in geothermal energy. Applied energy 2012, 98, 458-466.
21. Zhang, S.; Jiang, Z.; Zhang, S.; Zhang, Q.; Feng, G., Well placement optimization for large-scale geothermal energy exploitation considering nature hydro-thermal processes in the Gonghe Basin, China. Journal of Cleaner Production 2021, 317, 128391.
22. Liang, X.; Xu, T.; Feng, B.; Jiang, Z., Optimization of heat extraction strategies in fault-controlled hydro-geothermal reservoirs. Energy 2018, 164, 853-870.
23. Aliyu, M. D.; Chen, H.-P., Sensitivity analysis of deep geothermal reservoir: Effect of reservoir parameters on production temperature. Energy 2017, 129, 101-113.
24. Aliyu, M. D.; Chen, H.-P., Optimum control parameters and long-term productivity of geothermal reservoirs using coupled thermo-hydraulic process modelling. Renewable Energy 2017, 112, 151-165.
25. Jain, C.; Vogt, C.; Clauser, C., Maximum potential for geothermal power in Germany based on engineered geothermal systems. Geothermal Energy 2015, 3, 1-20.
26. Ma, W.; Xu, Y.; Ahmed, S. F.; Yang, C.; Liu, G., Techno-economic optimization of enhanced geothermal systems with multi-well fractured reservoirs via geothermal economic ratio. Energy 2024, 311, 133380.

27. Liu, S.; Liu, J.; Chai, J.; Xue, Y.; Liu, J.; Bai, X., Design and optimization of the U-shaped well geothermal systems for heat production performance: A case study from Huangling, China. Renewable Energy 2024, 223, 120060.
28. Gong, F.; Guo, T.; Sun, W.; Li, Z.; Yang, B.; Chen, Y.; Qu, Z., Evaluation of geothermal energy extraction in Enhanced Geothermal System (EGS) with multiple fracturing horizontal wells (MFHW). Renewable Energy 2020, 151, 1339-1351.
29. Yan, B.; Gudala, M.; Sun, S., Robust optimization of geothermal recovery based on a generalized thermal decline model and deep learning. Energy Conversion and Management 2023, 286, 117033.
30. Xie, J.; Wang, J., Numerical analysis and economic evaluation of pinnate horizontal well for supercritical CO2-based enhanced geothermal system. Geothermics 2024, 116, 102850.
31. Jiansheng, W.; Lide, S.; Qiang, Z.; Jintao, N., Numerical investigation on power generation performance of enhanced geothermal system with horizontal well. Applied Energy 2022, 325, 119865.
32. Sun, Y.; Zhang, X.; Liu, Y.; Zhang, X.; Li, X.; Sun, C.; Li, Z., Prediction and optimization of productivity and lifespan in multi-well enhanced geothermal system. Applied Thermal Engineering 2023, 234, 121155.
33. Maaref, S.; Shariat, A.; Joslin, K.; Novlesky, A. In Optimization of a Closed-Loop Geothermal System Under Different Operational Conditions, SPE Europec featured at EAGE Conference and Exhibition?, SPE: 2024; p D011S005R003.
34. Fontanilla, J. P.; Aziz, K., Prediction of bottom-hole conditions for wet steam injection wells. Journal of Canadian Petroleum Technology 1982, 21 (02).